

A Search for Photometric Rotation Periods in Low-Mass Stars and Brown Dwarfs in the Pleiades

Donald M. Terndrup,¹ Anita Krishnamurthi,²
 Marc H. Pinsonneault,¹

and

John R. Stauffer³

ABSTRACT

We have photometrically monitored (Cousins I_C) eight low mass stars and brown dwarfs which are probable members of the Pleiades. We derived rotation periods for two of the stars – HHJ409 and CFHT-PL8 – to be 0.258 d and 0.401 d, respectively. The masses of these stars are near 0.4 and 0.08 M_\odot , respectively; the latter is the second such object near the hydrogen-burning boundary for which a rotation period has been measured. We also observed HHJ409 in V ; the relative amplitude in the two bands shows that the spots in that star are about 200 K cooler than the stellar effective temperature of 3560 K and have a filling factor on the order of 13%. With one possible exception, the remaining stars in the sample do not show photometric variations larger than the mean error of measurement. We also examined the M9.5V disk star 2MASSJ0149, which had previously exhibited a strong flare event, but did not detect any photometric variation.

Subject headings: stars: low mass, brown dwarfs, rotation, activity; open clusters and associations: individual (Pleiades)

1. Introduction

During the last two decades, there have been many extensive studies of the rotation rates of G and K stars in open clusters (Stauffer et al. 1984, 1985, 1989; Stauffer & Hartmann 1987;

¹Department of Astronomy, The Ohio State University, Columbus, OH 43210; terndrup@astronomy.ohio-state.edu, pinsono@astronomy.ohio-state.edu.

²JILA, University of Colorado and National Institute of Standards and Technology, Boulder, CO 80309-0440; anitak@casa.colorado.edu.

³Smithsonian Astrophysical Observatory, 60 Garden Street, Cambridge, MA 02138; stauffer@amber.harvard.edu.

Stauffer et al. 1991; Soderblom et al. 1993; Krishnamurthi et al. 1998; Queloz et al. 1998), accompanied by considerable progress in understanding the mechanisms and mass dependence of angular momentum loss (see Pinsonneault 1997 for a review). Briefly, most stars arrive on the main sequence as relatively slow rotators, but about 20 - 25% arrive with rapid rotation ($20 < v \sin i < 200 \text{ km s}^{-1}$). The number of rapid rotators and the maximum observed rotation rates decline with increasing cluster age, showing that the time scale for these rapid rotators to lose most of their angular momentum ranges from tens to hundreds of millions of years, and that this time scale becomes longer with decreasing stellar mass. In order to be consistent with these observations, theoretical evolutionary models require one or more of the following features: (a) core-envelope rotational decoupling (Endal & Sofia 1981; Pinsonneault et al. 1990); (b) coupling of the stellar rotation to that of its circumstellar disk during pre-main sequence evolution (Königl 1991; Li & Collier Cameron 1993); and (c) saturation of the angular momentum loss rate above a specified rotation rate (Keppens et al. 1995).

Though the general trends are clear at higher masses, there is still not much information on the rotation rates of main sequence stars of low mass (here $M \leq 0.4M_{\odot}$). Jones et al. (1997), Stauffer et al. (1997), and Oppenheimer et al. (1997) have determined rotational velocities ($v \sin i$) for a small sample of stars in the Pleiades and Hyades with masses down to $\sim 0.1M_{\odot}$, while Basri & Marcy (1995) and Delfosse et al. (1998) have similarly obtained rotational velocities for low mass field stars. All of these studies indicate that the spindown time scales are longer for lower mass stars, with the time scale near $0.1 M_{\odot}$ being several billion years. This facet of the observational database is best explained by assuming that the critical rotation rate for saturation of the angular momentum loss rate is a function of mass (Krishnamurthi et al. 1997; Bouvier et al. 1997).

Obtaining more rotational data in the low-mass regime would help to constrain models of angular momentum evolution at the bottom of the main sequence. It would also be of interest to extend the samples into the substellar regime (“brown dwarfs”) to explore whether current formulations of angular momentum loss for stars are applicable there as well. Brown dwarfs are very low mass objects that do not burn hydrogen, and their properties are not very well characterized. Determining rotation rates for low-mass stars and substellar objects using high-resolution spectra is extremely challenging as they are quite faint ($I > 17$) and their spectra (late M-type) are complex. Furthermore, stars at and below the hydrogen-burning mass limit have quite small radii; the smallest rotation rates that are routinely determined spectroscopically (say $\approx 5 \text{ km s}^{-1}$), correspond to short rotation periods, about 0.5 day. Therefore the discovery of low-mass stars and brown dwarfs with periods in excess of 0.5 – 1 day may best be accomplished through photometry, which can detect brightness modulation from starspots. A determination of rotation periods by this method for brown dwarfs would indicate the presence of spots and hence magnetic activity on these sub-stellar objects, since the presence of starspots is a manifestation of magnetic fields.

Motivated by these considerations, we undertook a pilot study to derive rotation periods from

photometric modulation of low-mass members of the Pleiades. Section 2 describes the survey, and data analysis techniques, while § 3 presents our results and a discussion.

2. Observations and Analysis

We selected eight low-mass stars and brown dwarf candidates in the Pleiades; a list of these stars and a compilation of some of their properties is in Table 1. Columns 2–3 of that table show the J2000.0 positions for the targets, followed in columns 4–7, respectively, by their spectral classification and available photometry. The last two columns give a mass estimate, as derived from comparison to theoretical isochrones, and references for the various data about each star. The full sample ranges from $M \approx 0.4M_{\odot}$ down to $M \approx 0.05M_{\odot}$.

The two Pleiades stars with $M \approx 0.4M_{\odot}$, HHJ 409 and HHJ 375 (Hambly et al. 1993), were selected for monitoring because they are known to have quite different spectroscopic rotation rates of $v \sin i = 69 \text{ km s}^{-1}$ and 10 km s^{-1} , respectively (Stauffer et al. 1999). The rest of the stars were selected from deep imaging surveys which have produced candidate Pleiades brown dwarfs: Teide 1 (Rebolo et al. 1995), Teide 2 (Martín et al. 1998), Roque 11 and Roque 13 (Zapatero Osorio et al. 1997), and CFHT-PL-8 and CFHT-PL-12 (Bouvier et al. 1998).

A number of the fainter stars have spectra which show measurable equivalent widths of Li I $\lambda 6708 \text{ \AA}$. As originally proposed by Magazzù et al. (1993), stars with masses below about $0.065 M_{\odot}$ never develop central core temperatures sufficient to destroy lithium ($3 \times 10^6 \text{ K}$). At higher masses, the time it takes the core to achieve this temperature is a sensitive function of mass. Because low-mass stars are fully convective, the surface Li is rapidly depleted once the core reaches a high enough temperature. For clusters of the age of the Pleiades (100 – 120 Myr), the mass above which Li is depleted is about $0.08 M_{\odot}$ (Stauffer et al. 1998 and references therein); consequently, finding a Li abundance which does not show significant depletion would show that a given star in the Pleiades is a brown dwarf. The stars with spectroscopic confirmation of their status as brown dwarfs are Teide 1 (Rebolo et al. 1996), Teide 2 (Martín et al. 1998), Roque 13 and CFHT-Pl 12 (Stauffer et al. 1998).

We also monitored the very low-mass object 2MASS J0149090+295613 (hereafter referred to as 2MASSJ0149), which has exhibited a significant flare in $H\alpha$ (Liebert et al. 1999). As this flare can be interpreted as evidence for magnetic activity, we included this object in our sample to determine if we could observe spot modulation, which could be another indicator (or confirmation) of magnetic activity.

We used the 2.4-m Hiltner telescope of the MDM Observatory on Kitt Peak to obtain I_C (Cousins I band) photometry of our targets from UT 11-23 November 1998. The detector was the “Wilbur” CCD, a thick 2048×2048 Loral chip which was operated at a nominal gain of 2.3 electrons/DN and a readout noise of 4.7 electrons r.m.s. The readout was binned by a factor of two in rows and columns to yield a pixel scale of 0.393 arcseconds/pixel. In addition, we obtained a few

observations of HHJ 409 in V to measure the relative photometric amplitude at two wavelengths. Most of the run was photometric, with median seeing about $0.8''$; on a few nights we observed a large number of standards from Landolt (1992) for calibration, though in this paper we will only discuss amplitude variations and will not present calibrated photometry.

The EXPORT version of Sun/IRAF V2.11.1 for SunOS 4 and Solaris 2.6 was used for the initial processing of data. The raw images were corrected for overscan bias, zero-exposure level, and were flattened by twilight-sky flats. Inspection of the flats from several nights and of the sky level on deep exposures showed that the flattening process was accurate to 0.2% over most of the frames, increasing to about 1% at the extreme edges of the frames.

The observing strategy was to make repeated *visits* to each target and obtain from 2-5 exposures in quick succession; exposures ranged from 5-10 sec for the bright stars HHJ 375 and HHJ 409, and were as long as 300 sec for the faintest stars in the sample. Because the target fields were uncrowded, aperture photometry (rather than PSF-fitting) was adequate. Magnitudes were obtained for each unsaturated star on each frame in an aperture of radius 3 times the stellar FWHM; the median sky was measured in an annulus with radii of 5 and 7 times the FWHM.

The assembly of the magnitudes into a time series was accomplished in two steps. In the first, the magnitudes from the repeated exposures at each visit were averaged after rescaling by an additive constant. This offset was determined by shifting the stellar coordinates to a common system, then determining the mean weighted magnitude difference between photometry from pairs of frames, using all unsaturated stars common to each frame. The weights were assigned as $1/\sigma^2$, where σ was the magnitude error reported from the aperture photometry software. Because there were always a number of well-exposed stars on each frame, the magnitude offset could be determined very precisely (error typically ≤ 0.004 mag). The target star was included in the determination of the magnitude offset at this step because it would not have varied in the ≤ 30 min spent at each visit. The average HJD was taken as the time point for each visit.

In the second step, the average photometry for the many visits to each star were similarly scaled using mean weighted magnitude differences, but this time the target star was not included in the determination of the offset. Errors in the average magnitude were computed in both steps by taking the larger of the actual weighted error in the mean, or the expected error for Gaussian statistics.

Periods were determined using the Scargle (1982) implementation of the PERIODOGRAM algorithm for unevenly spaced data, which also yields the “false alarm probability” (FAP) that random fluctuations would produce the derived period. We also confirmed the derived periods (or absence of a detected signal) using the algorithm described in Roberts et al. (1987) (kindly supplied by D. H. Roberts), which takes into account aliasing introduced by the sampling frequency. Both algorithms yielded the same set of stars with definite detections and the resulting periods were the same.

3. Results and Discussion

The results of our observational program are summarized in Table 2. The first column lists the star names as in Table 1, while columns 2–5 show, respectively, the number of visits to the star, the r.m.s. scatter about the mean magnitude, and the average error in a single measurement. The last two columns display the derived period in days for the star and the false-alarm probability for the stars with definite periods.

As discussed in Section 2, the targets in our sample were selected to have a mass distribution which crossed the H-fusion boundary. We were able to measure definite rotation periods for two of the four low-mass stars (hydrogen burning) in our sample, namely HHJ 409 and CFHT-PL-8. The photometry for these two stars, phased to the derived period, is shown in Figures 1 and 2. Also shown on each figure is the photometry for a nearby star of similar brightness phased to the period of the target star; the scatter in the photometry of the nearby star is equal to the expected photometric error, verifying that the brightness variations in the target are real. In both figures, the differential photometry is plotted in the sense ($\Delta I_C = I_C - \langle I_C \rangle$). There is insufficient time-series data to be able to find a period for HHJ 375. This star shows photometric variation at the 2.5σ level, and a very approximate period of ~ 1.5 d (FAP ~ 0.4). CHFT-PL-8 has an amplitude of 10%; this star is comparable in mass to a star in the young cluster Alpha Perseii for which Martín & Zapatero Osorio (1997) derived a photometric rotation period. None of the other stars showed variations which were as much as twice the typical error of measurement (see table 2). Thus, we were unable to measure rotation periods for any of the objects which are likely to be sub-stellar.

We also followed HHJ 409 in V (five visits) to determine the relative amplitude compared to that in I_C . Figure 3 plots the difference in magnitude with respect to the average magnitude in each filter for these five visits. We find that the relative amplitude in V is 2.1 times that in I_C , and since the star gets redder as it gets fainter, the spots are cooler than the average temperature of the photosphere. The $V - I$ color of the star indicates a photospheric temperature of $T = 3560$ K. To estimate roughly the temperature difference between the spots and the star, we did a simple model of blackbody spots (see figure 4). For each assumed spot temperature, we derived a filling factor which would produce an amplitude of 0.04 mag in I_C ; the cooler the spots, the smaller the required filling factor to produce this amplitude. Then for each temperature, we calculated the resulting expected V amplitude. At spot temperatures near 3330 K and filling factors near 13%, the observed V amplitude of 0.08 mag was matched (Figure 4).

Though this measurement of the relative amplitudes in the two filters was only done for one star, it suggests that observations in wavelengths as red as I_C may be quite useful for this kind of work, for the simple reason that the stars are so much brighter in I than in V that it is easier to obtain good signal-to-noise in the photometry. Still, only two of our stars had amplitudes which were larger than the errors in the photometry. Several alternative explanations arise: the non-variables may have very little chromospheric activity, which is strongly correlated with

rotation (e.g., Krishnamurthi et al. 1998 and references therein). The stars may have activity cycles and it so happened that they did not have spots with a large filling factor during the time of our observations. Some higher-mass Pleiades stars show significant variations in their amplitude, which is interpreted as being the result of activity cycles (e.g., Stauffer et al. 1987b; Prosser et al. 1993), and our target J0149 has been quiescent except for the one flare event (Liebert et al. 1999). Finally, the spots may have very low contrast to the average photospheric color.

There have been several efforts recently to measure activity in brown dwarfs. Neuhäuser et al. (1999) conducted a search for X-ray emission from confirmed (Li test) and candidate brown dwarfs. A very small number of the targets were detected in X-rays: only one out of 26 brown dwarfs was detected, while 4 out of 57 of the brown dwarf candidates were detected. Except for 2MASSJ0149, the brown dwarfs and brown dwarf candidates studied in this paper were all included in the Neuhäuser et al. (1999) study. No detections were made and only upper limits were obtained for those of our targets included in that study.

This lack of activity is consistent with the findings of Krishnamurthi et al. (1999), who conducted a deep search for radio emission from a sample of very low mass stars and brown dwarfs in the field; no radio emission was detected from the studied targets. A possible explanation for a lack of detectable activity in such low-mass objects has been suggested by Neuhäuser et al. (1999) - brown dwarfs are fully convective objects that briefly burn deuterium and are not massive enough to burn hydrogen. When these objects stop burning deuterium, the core starts to cool down. As the temperature difference between the core and the surface decreases, the convective velocities decrease. This dampens the dynamo, which is powered not only by rotation, but also by the convection velocity. Thus, the objects may be rotating rapidly (as is seen from some measurements) but still not show much sign of activity in the form of X-ray emission, radio emission or spots.

In summary, we monitored a set of low-mass stars and brown dwarfs in the Pleiades and one low-mass star in the field in order to determine photometric rotational periods. We were able to derive rotation periods for two of the low mass stars. We thus verify (as in Martín & Zapatero Osorio 1997) that at least some stars near the hydrogen burning limit have large spot groups. The frequency of the spots is low (about 20-25%), or the spots have temperatures which are near that of the photosphere in these cool stars. We were unable to measure rotation periods for any of the (likely) substellar objects. From comparison to earlier work looking for activity, we speculate that this lack of detectable activity may be an inherent problem with using a sample of objects that are older than a few million years. If this hypothesis is correct, only very young brown dwarfs show signs of activity and it will be necessary to study such young objects to be able to detect spot activity. We will identify and study such candidates in an effort to determine if brown dwarfs show signs of magnetic activity at younger ages.

We acknowledge support from NSF grant AST-9731621 to MHP and DT. Thanks to MDM staff, and to Liam Mac Iomhair for his assistance at the telescope. AK received support from

NASA grant S-56500-D to the University of Colorado.

REFERENCES

- Basri, G., & Marcy, G. W. 1995, *AJ*, 109, 762
- Bouvier, J., Forrestini, M., & Allain, S. 1997, *A&A*, 326, 1023
- Bouvier, J., Stauffer, J. R., Martín, E. L., Barrado y Navascués, D., Wallace, B., & Béjar, V. J. S. 1998, *A&A*, 336, 490
- Delfosse, X., Forveille, T., Perrier, C., & Mayor, M. 1998, *A&A*, 331, 581
- Endal, A., & Sofia, S. 1981, *ApJ*, 243, 625
- Hambly, N. C., Hawkins, M. R. S., & Jameson, R. F. 1993, *A&AS*, 100, 607
- Jones, B. F., Fischer, D., Shetrone, M., & Soderblom, D. R. 1997, *AJ*, 114, 352
- Keppens, R., MacGregor, K. B., & Charbonneau, P. 1995, *A&A*, 294, 469
- Königl, A. 1991, *ApJ*, 370, L39
- Krishnamurthi, A., et al. 1998, *ApJ*, 493, 914
- Krishnamurthi, A., Leto, G., & Linsky, J. L. 1999, *AJ*, in press
- Krishnamurthi, A., Pinsonneault, M. H., Barnes, S., & Sofia, S. 1997, *ApJ*, 480, 303
- Landolt, A. U. 1992, *AJ*, 104, 340
- Li, J. & Collier Cameron, A. 1993, *MNRAS*, 261, 766
- Liebert, J., Kirkpatrick, J. D., Reid, I. N., & Fisher, M. D., 1999, *ApJ*, in press
- Magazzù, A., Martín, E. L., & Rebolo, R. 1993, *ApJ*, 404, L17
- Martín, E. L., Basri, G., Gallegos, J. E., Rebolo, R., Zapatero Osorio, M. R., & Bejar, V. J. S. 1998, *ApJ*, 499, L61
- Martín, E. L., & Zapatero Osorio, M. R. 1997, *MNRAS*, 286, L17
- Neuhäuser, R., Briceño, C., Comerón, F., Hearty, T., Martín, E. L., Schmitt, J. H. M. M., Stelzer, B., Supper, R., Voges, W., & Zinnecker, H. 1999, *A&A*, 343, 883
- Oppenheimer, B., Basri, G., Nakajima, T., & Kulkarni, S. 1997, *AJ*, 113, 296
- Pinsonneault, M. H. 1997, *ARA&A*, 35, 557

- Pinsonneault, M., Kawaler, S. D., & Demarque, P. 1990, *ApJS*, 74, 501
- Prosser, C. F., Schild, R. E., Stauffer, J. A., & Jones, B. F. 1993, *PASP*, 105, 269
- Queloz, D., Allain, S., Mermilliod, J.-C., Bouvier, J., & Mayor, M. 1998, *A&A*, 335, 183
- Rebolo, R., Martín, E. L., Basri, G., Marcy, G. W., & Zapatero Osorio, M. R. 1996, *ApJ*, 469, L53
- Rebolo, R., Zapatero Osorio, M. R., & Martín, E. L. 1995, *Nature*, 377, 129
- Roberts, D. H., Lehár, J., & Dreher, J. W. 1987, *AJ*, 93, 968
- Scargle, J. D. 1982, *ApJ*, 263, 853
- Soderblom, D., Stauffer, J., Hudon, D. & Jones, H. 1993, *ApJS*, 85, 315
- Stauffer, J. R., Balachandran, S. C., Krishnamurthi, A., Pinsonneault, M., Terndrup, D. M., & Stern, R. A. 1997, *ApJ*, 475, 604
- Stauffer, J. R., Giampapa, M. S., Herbst, W., Vincent, J. M., Hartmann, L. W., & Stern, R. A. 1991, *ApJ*, 374, 142
- Stauffer, J. R., & Hartmann, L. W. 1987, *ApJ*, 318, 337
- Stauffer, J. A., Hartmann, L. W., Burnham, J. N., & Jones, B. F. 1985, *ApJ*, 289, 247
- Stauffer, J. A., Hartmann, L. W., & Latham, D. W. 1987a, *ApJ*, 320, 51
- Stauffer, J. R., Hartmann, L., Soderblom, D. R., & Burnham, N. 1984, *ApJ*, 280, 202
- Stauffer, J. A., Schild, R. E., Baliunas, S. L., & Africano, J. L. 1987b, *PASP*, 99, 471
- Stauffer, J. R., Schultz, G., & Kirkpatrick, J. D. 1998, *ApJ*, 499, L199
- Stauffer, J. R., Terndrup, D. M., Pinsonneault, M. H., Sills, A., Yuan, Y., Jones, B. F., Fischer, D., & Krishnamurthi, A. 1999, *ApJ*, in preparation
- Zapatero Osorio, M. R., Rebolo, R., Martín, E. L., Basri, G., Magazzù, A., Hodgkin, S. T., Jameson, R. F., & Cossburn, M. R. 1997, *ApJ*, 491, L81
- Zapatero Osorio, M. R., Rebolo, R., Martín, E. L., Hodgkin, S. T., Cossburn, M. R., Magazzù, A., Steele, I. A., & Jameson, R. F. 1999, *A&AS*, 134, 537

Table 1. Characteristics of observed targets

Name	RA (2000)	Dec (2000)	Spectral type	I	$I - K$	Mass (M_{\odot}) ^a	Reference ^b
2MASSJ0149	01:49:09.0	+29:56:13	M9.5V	...	1.40	...	L
Roque 11	03:47:12.1	+24:28:32	M8	18.75	3.63	0.06	Z3
Roque 13	03:45:50.6	+24:09:03	M7.5	18.25	3.65	0.07	Z3
Teide 1	03:47:18.0	+24:22:31	BD	18.80	3.69	0.055	Z1
Teide 2	03:52:06.7	+24:16:01	M6	17.82	...	0.072	M
HHJ 375	03:48:05.8	+23:02:04	...	13.74	...	0.39	H,S
HHJ 409	03:42:40.2	+23:59:22	...	13.34	...	0.39	H,S
CFHT-PL8	03:42:26.8	+24:50:21	...	17.42	...	0.084	B
CFHT-PL12	03:53:55.1	+23:16:01	...	18.02	...	0.070	B

^aMasses estimated from photometry; see references.

^bReferences: (B) Bouvier et al. (1998); Hambly et al. (1993); (L) Liebert et al. (1999); (M) Martín et al. (1998); (S) Stauffer et al. 1999; (Z1) Zapatero Osorio et al. (1997); (Z3) Zapatero Osorio et al. (1999).

Table 2. Results

Name	Visits	r.m.s ΔI_C	mean error	period (day)	FAP
2MASSJ0149	37	0.014	0.011
Roque 11	27	0.041	0.043
Roque 13	21	0.023	0.025
Teide 1	25	0.045	0.027
Teide 2	31	0.018	0.014
HHJ 375	18	0.007	0.004
HHJ 409	32	0.015	0.004	0.258	3.5×10^{-4}
CFHT-PL8	34	0.028	0.007	0.401	5.7×10^{-4}
CFHT-PL12	32	0.016	0.012

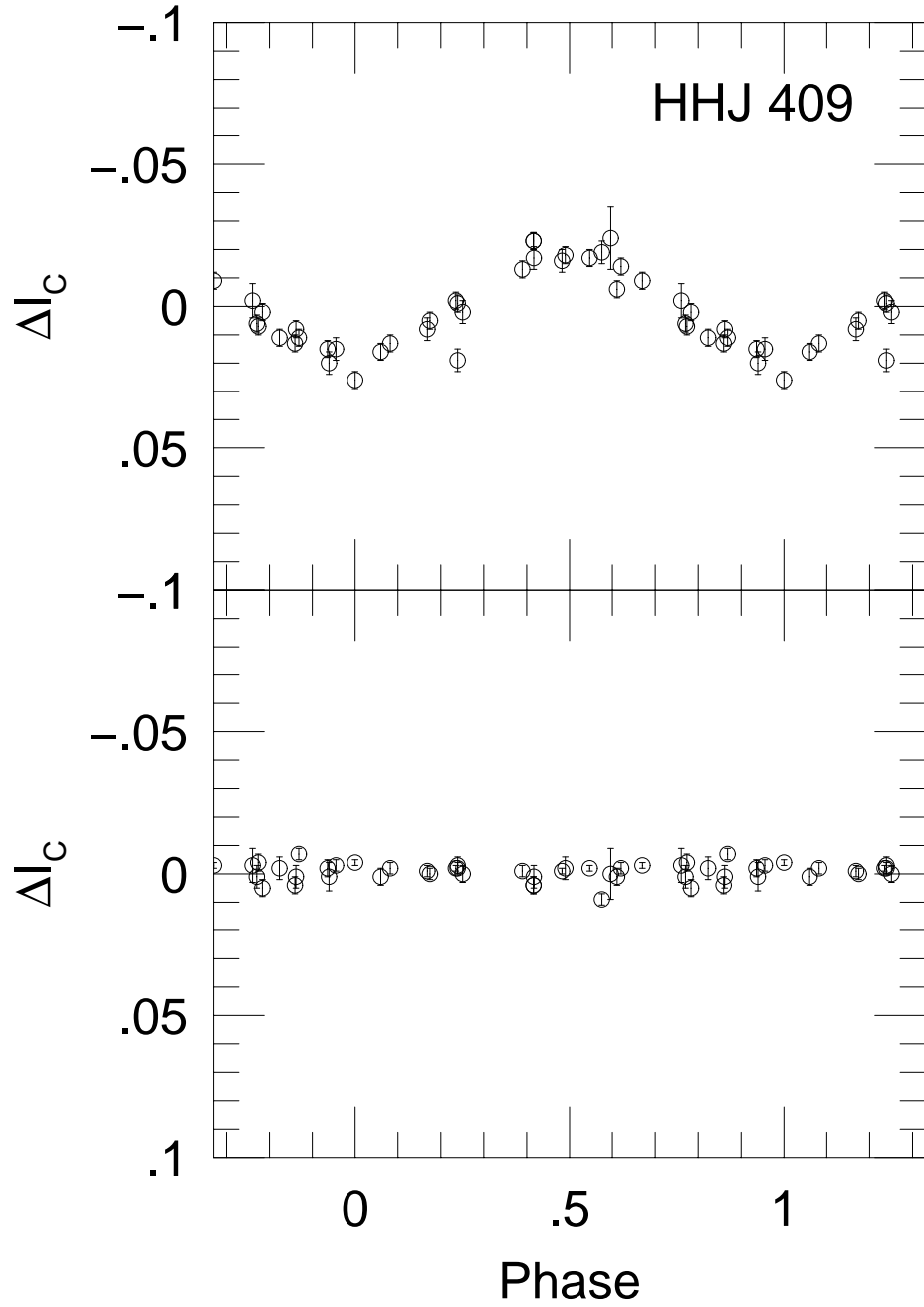


Fig. 1.— Photometry for HHJ 409 (upper panel) and for a nearby star of similar brightness (lower panel), both phased to the derived period of 0.258 d.

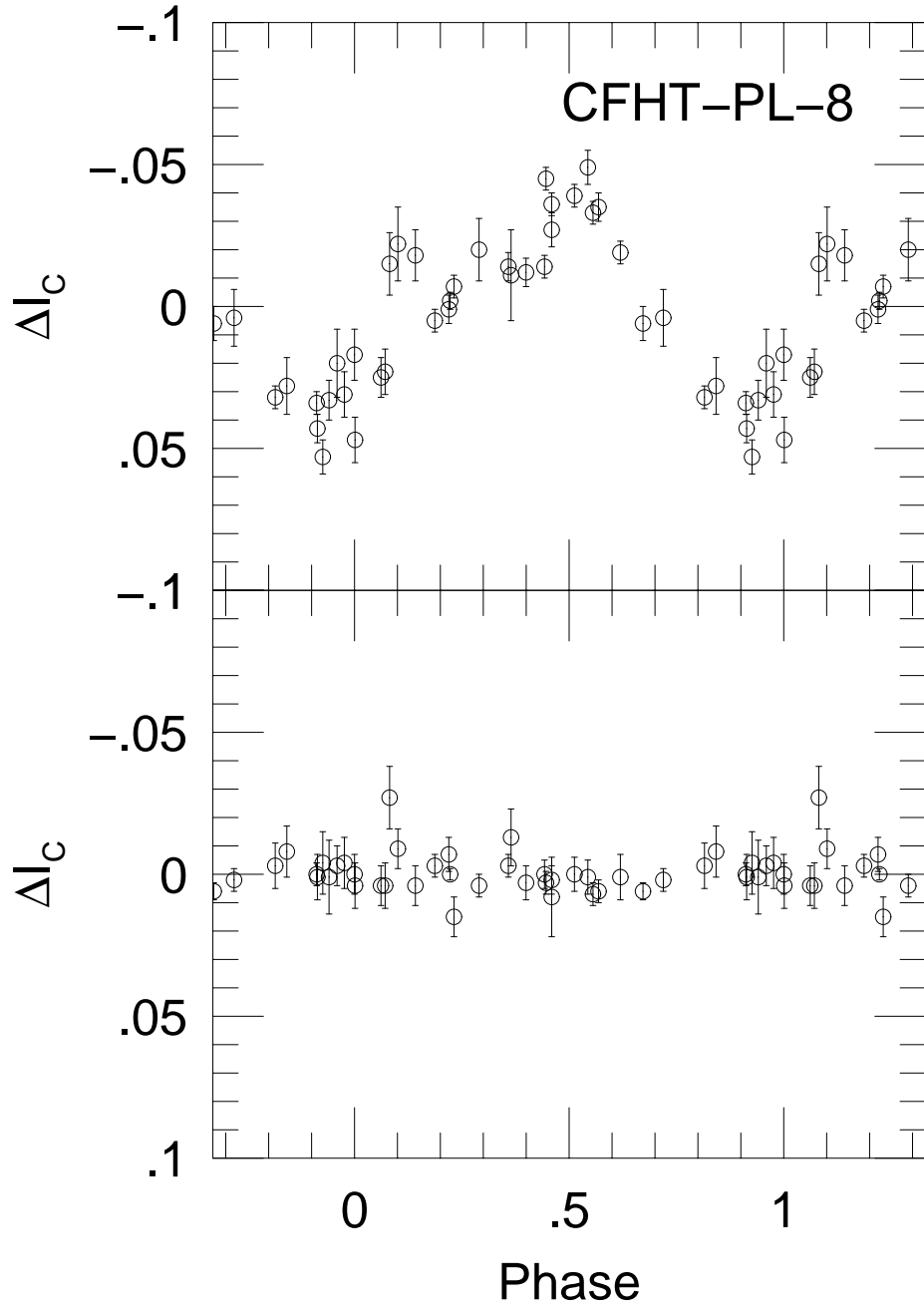


Fig. 2.— Same as Figure 1, but for CFHT-PL-8. The phasing is for the derived period of $P = 0.402$ d.

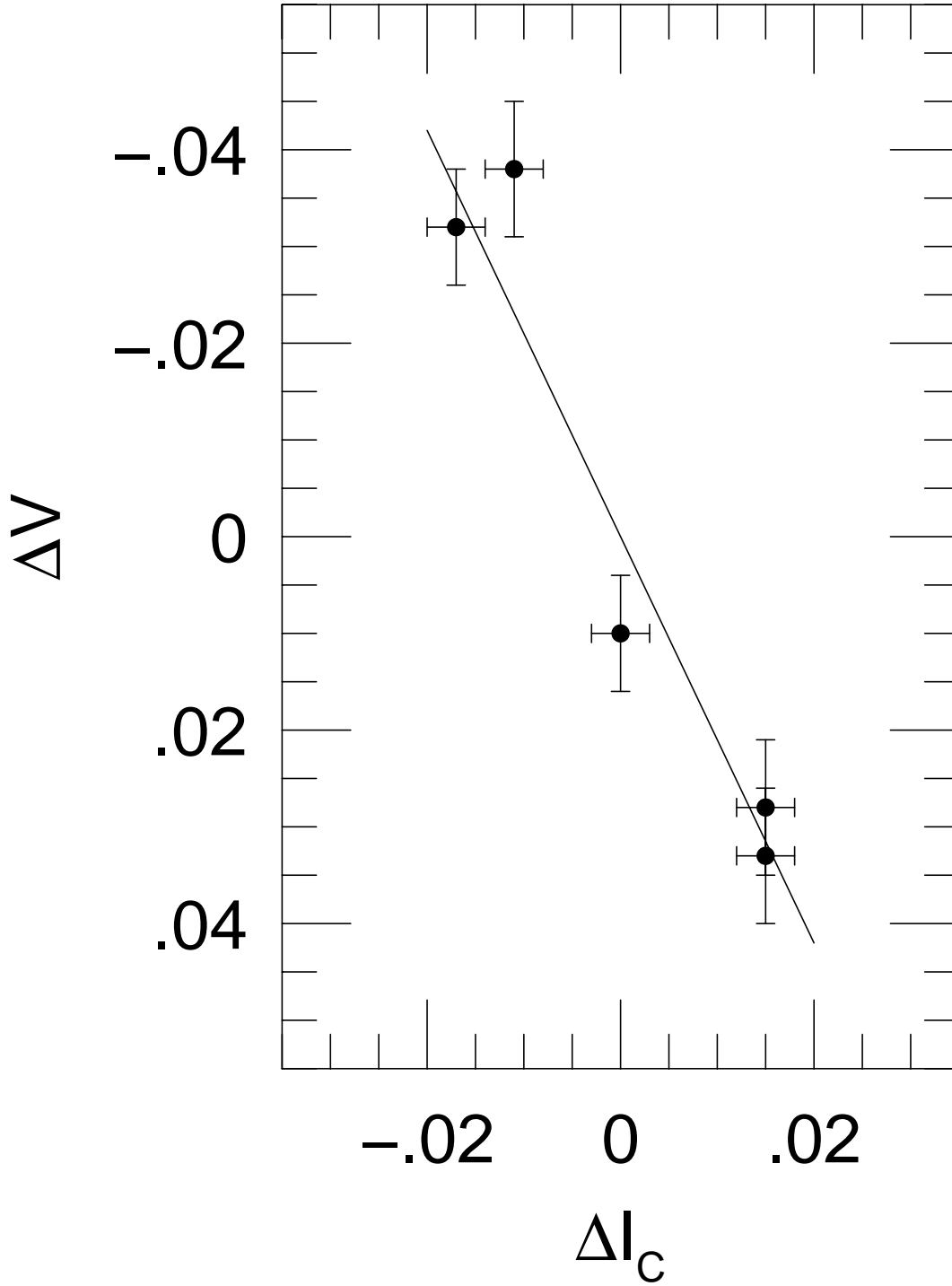


Fig. 3.— Differential photometry in V and I_C for HHJ 409, where the values are in the sense magnitude - mean. The solid line is a linear fit to the data; the amplitude in V is 2.1 times that in I_C . The star becomes redder as it gets fainter, showing that the spots are cooler than the photosphere.

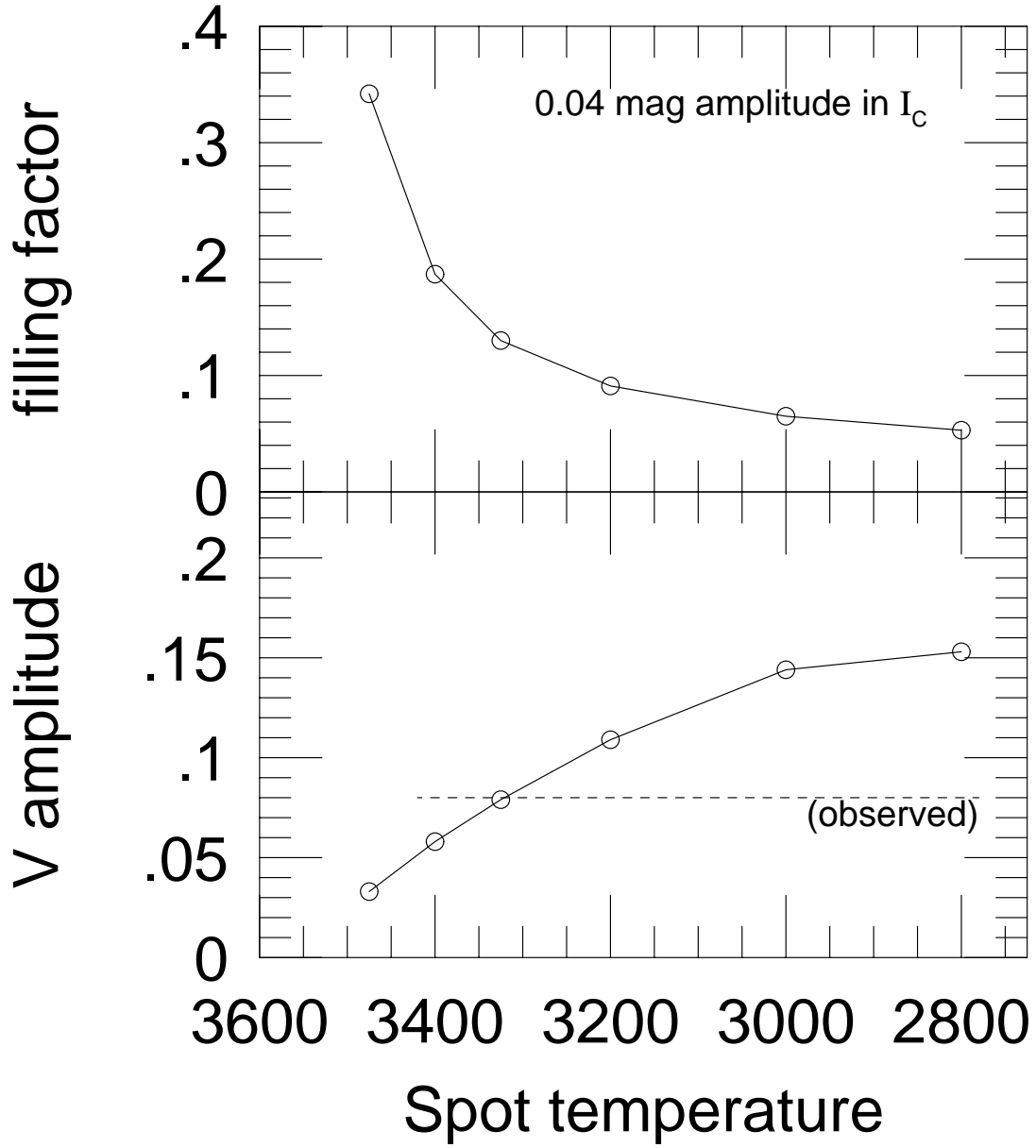


Fig. 4.— Simple model of blackbody spots for HHJ 409: top panel shows the filling factor required to produce a 4% variation in I_C for different spot temperatures. The bottom panel shows the expected V amplitude for different spot temperatures. The spot temperature for HHJ 409 is taken to be that which corresponds to the observed V amplitude of 0.08 magnitude, or 3330K. This also corresponds to a filling factor of $\sim 13\%$ from the top panel.